

A Library of SIMULINK Blocks for Real-Time Control of HEV Traction Drives

John Chiasson¹, Leon Tolbert^{1,2}

¹The University of Tennessee

²Oak Ridge National Laboratory

Copyright © 2002 Society of Automotive Engineers, Inc.

ABSTRACT

This paper describes the development of advanced control and modeling algorithms for the various types of motor drives considered for hybrid electric vehicles (HEVs). The algorithms are given in the high-level language of MATLAB/SIMULINK. The algorithms consist of SIMULINK blocks that can be easily implemented in a real-time test environment for induction, switched reluctance, and permanent magnet synchronous machines. This eliminates the need for specialized programming in C or assembly languages providing investigators a much simpler way to study proposed control algorithms for various motor drives.

INTRODUCTION

This paper describes the development of a SIMULINK library of control and modeling algorithms for the various types of motor drives considered for hybrid electric vehicles (HEVs). The algorithms are given in the high-level language SIMULINK from Mathworks Inc. The algorithms consist of SIMULINK blocks that can be easily implemented in a real-time test environment for induction, switched reluctance, and permanent magnet synchronous machines. This eliminates the need for specialized programming in C or assembly languages providing investigators a much simpler way to study proposed control algorithms for various motor drives.

The components of a HEV include an internal combustion engine, an AC motor/generator, a battery and power electronics. From the electrical point of view, a major concern is the challenge of using an inverter (power electronics) to convert the battery power to the appropriate time-varying voltages required by the electric motor to produce torque for the vehicle's propulsion.

Presently, researchers have considered several motor types including the DC motor, induction motor, permanent magnet (PM) synchronous motor, and the switched reluctance (SR) motor. Each of these motors are quite different in their operation, and each requires a specialized computer controller (software program) to determine when the electronic switches of the power inverter should switch to produce the appropriate voltage for the motor. The issue of which

motor to use for the propulsion of electric vehicles is still unresolved because the cost, performance, reliability, size, and efficiency all play a large role in the decision and no one motor can presently be said to be the "best" choice (The dc motor has been ruled out due to its higher cost and higher maintenance requirements.). Consequently, having a library of various motor models and controllers is advantageous for the development of HEVs.

The approach here is to do the control system design software using MATLAB/SIMULINK which allows one not only to design a controller for the system using block diagrams (on the design PC), but it also provides the capability to convert the block diagram to executable code which is then downloaded to be run on a real-time PC. That is, the software program RTW[®] (real-time workshop) converts the SIMULINK diagram to C code and then this can be converted to real-time executable code. The I/O (input/output) interface boards read in the information (voltages, currents, speed, position, temperature, etc.) from the motor needed by the control program and sends out the commands to the power electronics as determined by the control program. This approach eliminates the need for specialized programming in C or Assembly Languages, and instead allows investigators to spend their time intensively studying the proposed control algorithms¹.

Basic SIMULINK Libraries are developed for the switched reluctance, PM synchronous and induction motors.

REAL-TIME TEST BED

A real-time computing platform has been developed as a test bed to efficiently and accurately carry out the real-time implementation of sophisticated computer algorithms for the control of any of the possible alternatives for the propulsion of the electric vehicle. As shown in the Figure below, this platform consists of three

¹ An appropriate analogy is the typewriter versus the word processor. The ability to do work with a word processor (correspondingly, a real-time setup) greatly decreases the turn around time and increases the possibilities compared with using a typewriter (C or Assembly Language Programming).

personal computers (PCs) in which one serves as “host” PC for the development/design using SIMULINK and the other two “target” PCs are used to run in real-time to serve as the controller for the motor/inverter. There are various 3rd party vendors who provide the capability to convert the SIMULINK generated C-code to real-time executable code. We chose the real-time implementation platform using RTLAB[®] from Opal RT Technologies 1 since it provides a high performance solution from off the shelf equipment making it relatively a low cost approach. The two target PCs allow one to different parts of the controller at different rates. In particular, one target PC can run with a 50-microsec step size for the power electronic inverter controller and the other with a 200-microsec step size for the motor controller.

the difficulty in its control. Unlike induction, synchronous, and DC motors, the characterization (mathematical model) of the SR motor is quite difficult to determine and work with to develop control algorithms. This is due to the fact that its flux/torque model is a non-parametric nonlinear function of the motor current and position. Consequently, this function must be determined in tabular form.

As a first example, it is shown how the evaluation platform can be a powerful tool to automatically characterize (model) and control a SR motor drive system for HEVs. The basic library consists of computer algorithms (SIMULINK programs) provide.

Automatic identification of the i^{th} phase torque function $\tau_i(n_R\theta, i)$.

Automatic identification of R_s, J .

A motor controller (software algorithm) that determines the currents i_a, i_b, i_c needed at each instant in time so that the motor produces the requisite torque.

The basic mathematical model of a three-phase switched reluctance motor is given by

$$\frac{d}{dt} \lambda_1(n_R\theta, i_1) = -R_s i_1 + u_1 \quad (1)$$

$$\frac{d}{dt} \lambda_2(n_R\theta, i_2) = -R_s i_2 + u_2 \quad (2)$$

$$\frac{d}{dt} \lambda_3(n_R\theta, i_3) = -R_s i_3 + u_3 \quad (3)$$

$$J \frac{d\omega}{dt} = \tau - \tau_L \quad (4)$$

$$\tau = \tau_1(n_R\theta, i_1) + \tau_2(n_R\theta, i_2) + \tau_3(n_R\theta, i_3) \quad (5)$$

$$= \frac{\partial}{\partial \theta} \left(\int_0^{i_1} \lambda_1(n_R\theta, i) di + \int_0^{i_2} \lambda_2(n_R\theta, i) di + \int_0^{i_3} \lambda_3(n_R\theta, i) di \right) \quad (6)$$

Here $\lambda_i, i_i, u_i, i = 1,2,3$ are, respectively, the fluxes, currents and voltages in the three stator phases. This is written in nonlinear state-space form as

$$\frac{di_1}{dt} = \left(-R_s i_1 - \frac{\partial \lambda_1(n_R\theta, i_1)}{\partial \theta} n_R \omega + u_1 \right) / \frac{\partial \lambda_1(n_R\theta, i)}{\partial i} \quad (7)$$

$$\frac{di_2}{dt} = \left(-R_s i_2 - \frac{\partial \lambda_2(n_R\theta, i_2)}{\partial \theta} n_R \omega + u_2 \right) / \frac{\partial \lambda_2(n_R\theta, i)}{\partial i} \quad (8)$$

$$\frac{di_3}{dt} = \left(-R_s i_3 - \frac{\partial \lambda_3(n_R\theta, i_3)}{\partial \theta} n_R \omega + u_3 \right) / \frac{\partial \lambda_3(n_R\theta, i)}{\partial i} \quad (9)$$

$$J \frac{d\omega}{dt} = \tau(n_R\theta, i_1, i_2, i_3) - \tau_L \quad (10)$$

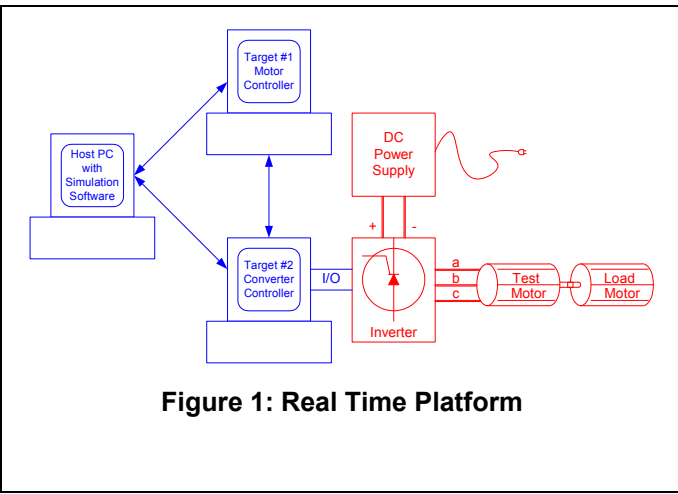


Figure 1: Real Time Platform

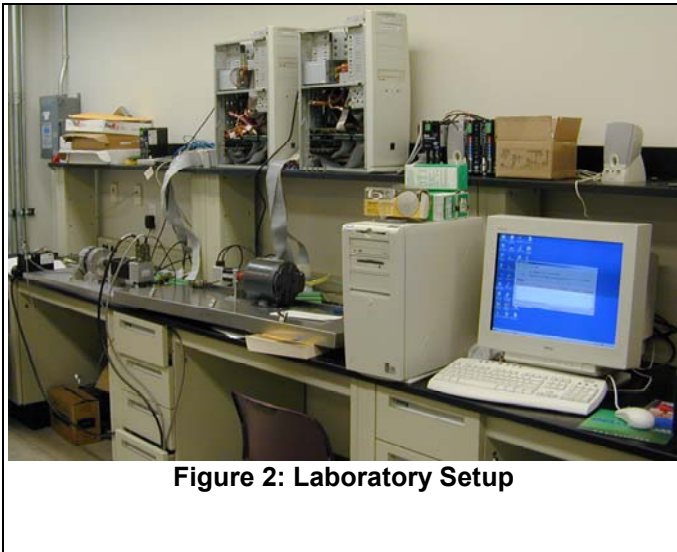


Figure 2: Laboratory Setup

THE SWITCHED RELUCTANCE MOTOR

The Switched Reluctance (SR) Motor has been proposed as an alternative for electrical vehicle propulsion due its simple structure making it not only cheap to manufacture, but rugged and durable. However, this advantage is currently overshadowed by

Clicking on the **Phase Current Command and their Torques** block gives the fourth level shown in Figure 6.

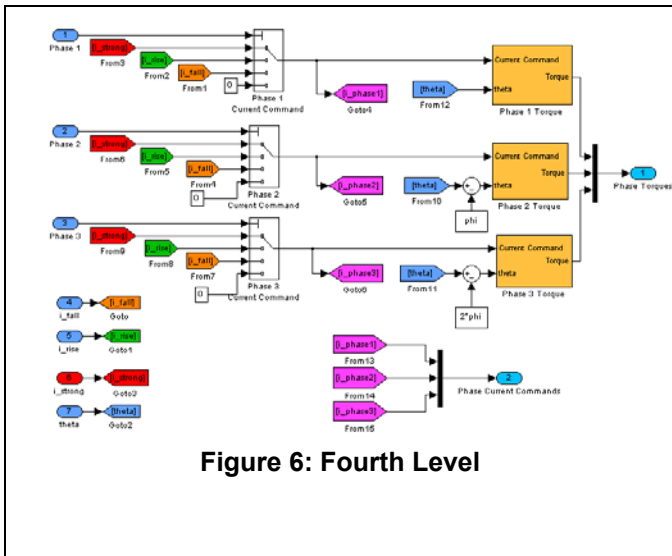


Figure 6: Fourth Level

Finally, clicking on the **Phase 1 Torque** block gives the fifth level of the model shown in Figure 7.

The point here is to show that complexity involved in such controllers. The complete controller is developed off line in

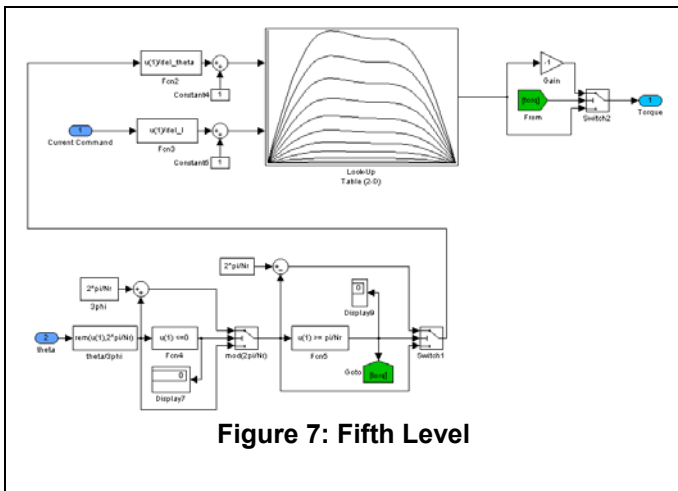


Figure 7: Fifth Level

simulation. Then, one removes the motor model and replaces them with the RTLAB (Opal RT) I/O blocks icons (or a similar 3rd party vendor's software icons) to communicate with the A/Ds, D/As, encoder, and digital I/O. Then one compiles the SIMULINK model into C code using RTW that is then converted into executable code using RTLAB (Opal RT, Inc.) software. The look up table in the above figure shows the torque $\tau_r(n_R\theta, i_{1r})$ as a function of position for various current levels. Such a table is found experimentally. A SIMULINK model was developed to automatically identify the function $\tau_r(n_R\theta, i_{1r})$ and the experimental results for an eight-pole rotor switched reluctance motor are shown in the figure below.

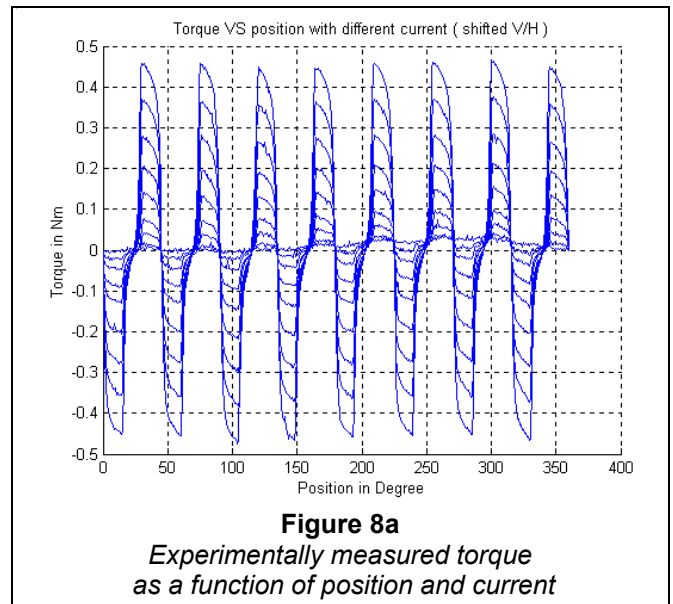


Figure 8a
Experimentally measured torque as a function of position and current

This was an automatic identification procedure in which the position of load motor is incremented in steps of $360^\circ/400 = .09^\circ$ starting at zero going to a full 360° turn of the motor. With a constant current in phase 1 of the SR motor, the torque is measured using a torque sensor placed between the test motor and load motor. This procedure is automatically repeated for 10 current levels in steps of $2.5A/10 = .25 A$ resulting in Figure 8.

The data of Figure 8 for just one positive torque cycle is given Figure 8b below. Figure 8 is the data that goes in the lookup table shown in Figure 7.

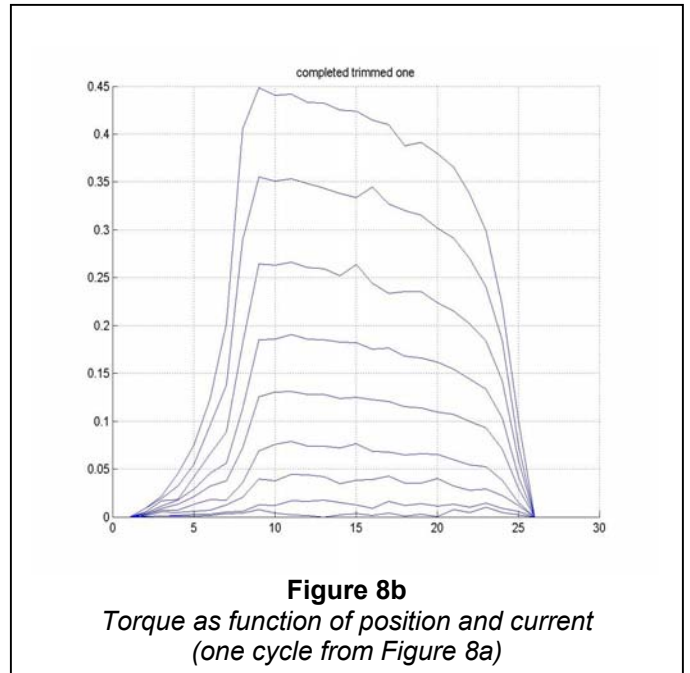


Figure 8b
Torque as function of position and current (one cycle from Figure 8a)

The data of Figure 8 is inverted to obtain the phase current as a function of position and torque which is needed by the controller. That is, given the rotor position and the torque, the current in the phase required to get the torque is given in Figure 8c. The Simulink feedback controller outlined above was then converted for real-time implementation using RTLAB (Opal RT, Inc.) software. A trajectory was chosen to have the motor go up to 50rad/sec and then come back down to rest. The actual data of the speed tracking is shown in Figure 8d.

In this figure, the speed was computed by backward differentiation of the encoder position measurement and the granularity in the speed is simply due to the resolution of the encoder. The position was also tracked and is shown in Figure 8e along with its reference trajectory. The error in the position tracking is small enough that it is not discernible in this figure. The current tracking is also shown below for one of the phases. This particular implementation used current command amplifiers and the figure indicates that the amplifier was not able to track the commanded currents with zero steady-state error. In fact, further investigation showed that the amplifiers low bandwidth prevented the controller from tracking high speed trajectories. The authors are now developing methods to get around this difficulty.

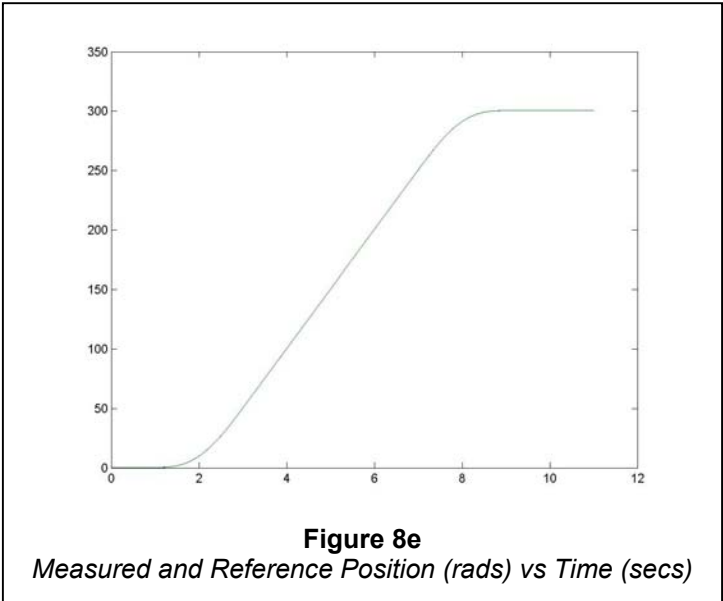


Figure 8e
Measured and Reference Position (rads) vs Time (secs)

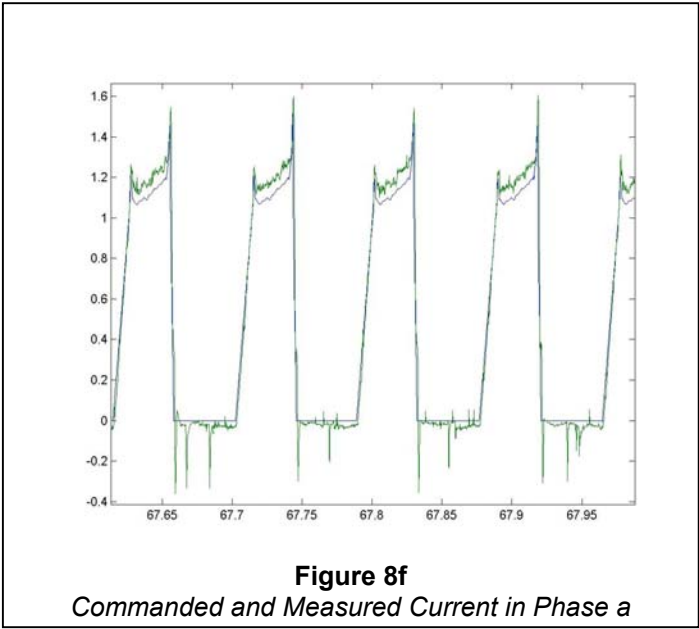


Figure 8f
Commanded and Measured Current in Phase a

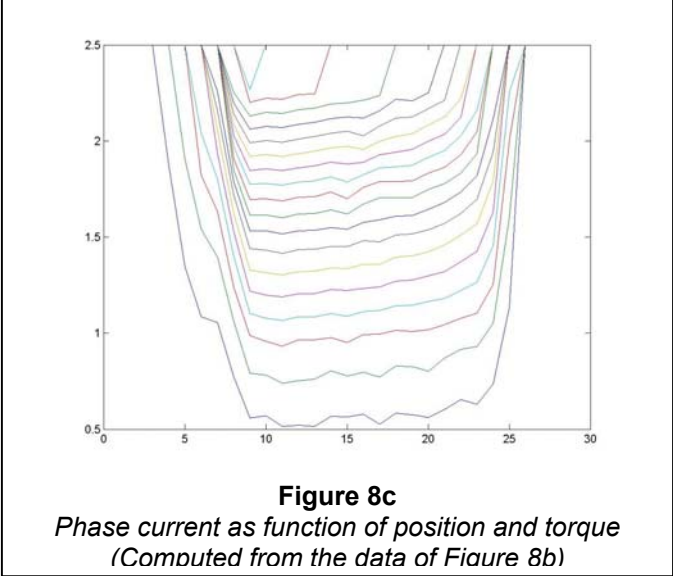


Figure 8c
Phase current as function of position and torque
(Computed from the data of Figure 8b)

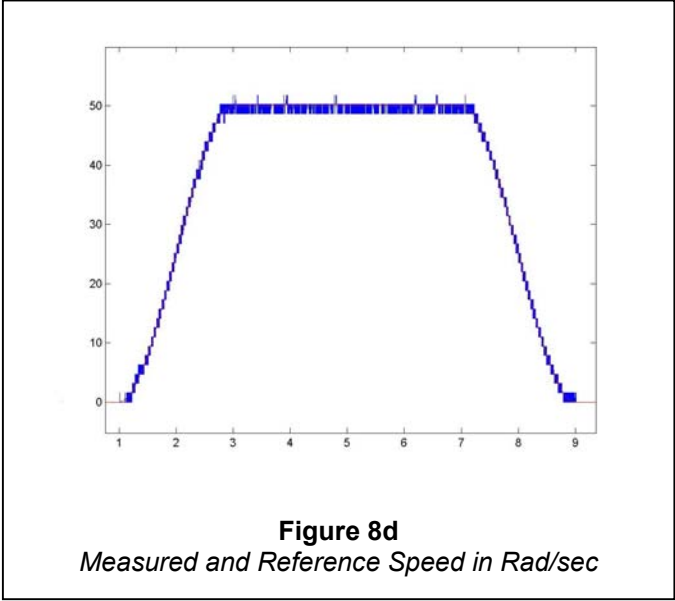


Figure 8d
Measured and Reference Speed in Rad/sec

SYNCHRONOUS MOTOR

A basic Library of SIMULINK blocks has also been developed for the PM synchronous motor. The standard model of the 3 phase PM synchronous motor is

$$L_S \frac{di_{S1}}{dt} - M \frac{di_{S2}}{dt} - M \frac{di_{S3}}{dt} = v_{S1} - Ri_{S1} + K_m \omega \sin(n_p \theta) \tag{18}$$

$$-M \frac{di_{S1}}{dt} + L_S \frac{di_{S2}}{dt} - M \frac{di_{S3}}{dt} = v_{S2} - Ri_{S2} + K_m \omega \sin\left(n_p \theta - \frac{2\pi}{3}\right) \tag{19}$$

$$-M \frac{di_{S1}}{dt} - M \frac{di_{S2}}{dt} + L_S \frac{di_{S3}}{dt} = v_{S3} - Ri_{S3} + K_m \omega \sin\left(n_p \theta - \frac{4\pi}{3}\right) \quad \sqrt{3}(L_S - 2M) \frac{di_0}{dt} = v_0 - Ri_0 \quad (29)$$

$$J \frac{d\omega}{dt} = -K_m i_{S1} \sin(n_p \theta) - K_m i_{S2} \sin\left(n_p \theta - \frac{2\pi}{3}\right) - K_m i_{S3} \sin\left(n_p \theta - \frac{4\pi}{3}\right) - \tau_L \quad J \frac{d\omega}{dt} = -K i_a \omega \sin(n_p \theta) + K i_b \cos(n_p \theta) - \tau_L \quad (30)$$

where L_S is the self-inductance of a stator winding, M is the coefficient of mutual inductance between the phases, K_m is the torque/back-emf constant, R is the resistance of a stator winding, J is the moment of inertia of the rotor, τ_L is the load torque, θ is the rotor angular position, ω is the rotor speed and n_p is the number of pole pairs (or the number of rotor teeth for a stepper motor). If the phases were perfectly coupled, one would have $M = L_S/2$.

The power preserving *three-phase to two-phase transformation* is defined by

$$\begin{bmatrix} i_a \\ i_b \\ i_0 \end{bmatrix} \equiv \sqrt{\frac{2}{3}} \begin{bmatrix} 1 & -1/2 & -1/2 \\ 0 & \sqrt{3}/2 & -\sqrt{3}/2 \\ 1/\sqrt{2} & 1/\sqrt{2} & 1/\sqrt{2} \end{bmatrix} \begin{bmatrix} i_{S1} \\ i_{S2} \\ i_{S3} \end{bmatrix} \quad (22)$$

$$\begin{bmatrix} v_a \\ v_b \\ v_0 \end{bmatrix} \equiv \sqrt{\frac{2}{3}} \begin{bmatrix} 1 & -1/2 & -1/2 \\ 0 & \sqrt{3}/2 & -\sqrt{3}/2 \\ 1/\sqrt{2} & 1/\sqrt{2} & 1/\sqrt{2} \end{bmatrix} \begin{bmatrix} v_{S1} \\ v_{S2} \\ v_{S3} \end{bmatrix} \quad (23)$$

and transforms the original model into the equivalent model

$$(L_S + M) \frac{di_a}{dt} = v_a - Ri_a + \sqrt{\frac{3}{2}} K_m \omega \sin(n_p \theta) \quad (24)$$

$$(L_S + M) \frac{di_b}{dt} = v_b - Ri_b + \sqrt{\frac{3}{2}} K_m \omega \sin(n_p \theta) \quad (24)$$

$$(L_S + M) \frac{di_0}{dt} = \frac{1}{\sqrt{3}} v_0 - \frac{1}{\sqrt{3}} Ri_0 \quad (25)$$

$$J \frac{d\omega}{dt} = -\sqrt{\frac{3}{2}} K_m i_a \sin(n_p \theta) + \sqrt{\frac{3}{2}} K_m i_b \cos(n_p \theta) - \tau_L \quad (26)$$

Under balanced operation in which $v_0 = v_{S1} + v_{S2} + v_{S3} = 0$, $i_0 = i_{S1} + i_{S2} + i_{S3} = 0$, one obtains the two-phase equivalent model given by

$$L \frac{di_a}{dt} = v_a - Ri_a + K \omega \sin(n_p \theta) \quad (27)$$

$$L \frac{di_b}{dt} = v_b - Ri_b - K \omega \sin(n_p \theta) \quad (28)$$

where $L = L_S + M$ (approximately $K = \sqrt{3/2} K_m$, $3L_S/2$), i_a and i_b are the equivalent currents in phases *a* and *b*, respectively.

Letting V_{bus} denote the DC bus voltage of a 3-phase inverter, the maximum voltage out of the inverter is obtained in six step mode, resulting in a peak of the fundamental waveform equal to $v_{max} = (2/\pi) V_{bus}$, which is the maximum phase voltage. With i_{max} and v_{max} denoting the limits of the 3-phase currents and voltages, respectively, the corresponding limits I_{max} , V_{max} for the equivalent 2-phase motor are $I_{max} = \sqrt{\frac{3}{2}} i_{max}$,

$V_{max} = \sqrt{\frac{3}{2}} v_{max} = \sqrt{\frac{3}{2}} \frac{2}{\pi} V_{bus}$. The *direct-quadrature* or *dq* transformation is given by

$$\begin{bmatrix} i_d \\ i_q \end{bmatrix} = \begin{bmatrix} \cos(n_p \theta) & \sin(n_p \theta) \\ -\sin(n_p \theta) & \cos(n_p \theta) \end{bmatrix} \begin{bmatrix} i_a \\ i_b \end{bmatrix} \quad (31)$$

$$\begin{bmatrix} v_d \\ v_q \end{bmatrix} = \begin{bmatrix} \cos(n_p \theta) & \sin(n_p \theta) \\ -\sin(n_p \theta) & \cos(n_p \theta) \end{bmatrix} \begin{bmatrix} v_a \\ v_b \end{bmatrix} \quad (32)$$

where i_d , i_q and v_d , v_q are the transformed currents and voltages respectively, in the *dq* (for direct and quadrature) reference frame. The state-space model in the *dq* coordinates is

$$L \frac{di_d}{dt} = v_d - Ri_d + n_p \omega Li_q \quad (33)$$

$$L \frac{di_q}{dt} = v_q - Ri_q - n_p \omega Li_d - K \omega \quad (34)$$

$$J \frac{d\omega}{dt} = K i_q - \tau_L \quad (35)$$

$$\frac{d\theta}{dt} = \omega \quad (36)$$

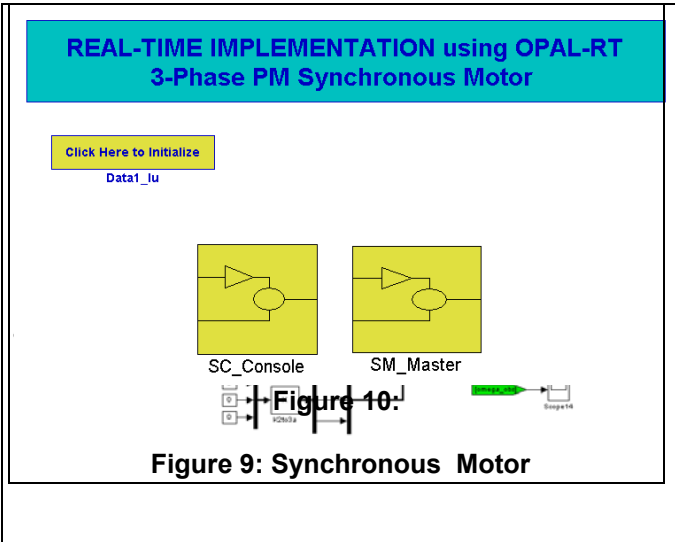
A standard controller is then

$$v_q = K_p (i_{dref} - i_d), i_{dref} = 0 \quad (37)$$

$$v_d = K_p (i_{qref} - i_q), i_{qref} = \tau_{ref} / K \quad (38)$$

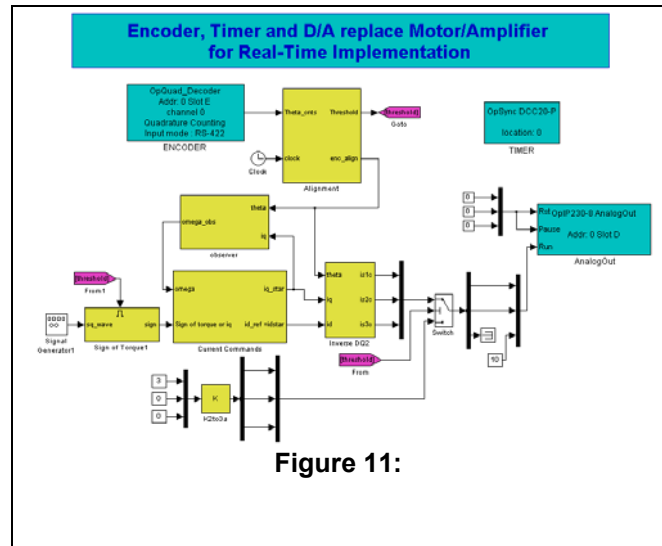
Such a model is shown in the figure below using standard field-oriented implementation. The simulation of

the motor is shown on the right side while the simulation of the controller is shown on the left side.



To illustrate the how such a standard off line Simulink simulation is converted to real-time, the first step is shown in the figure below. The block labeled **SM_Master** contains the controller blocks from the above figure.

In more detail, clicking on this block gives the block diagram below. This should be compared with first figure in this section as appropriate I/O blocks have replaced

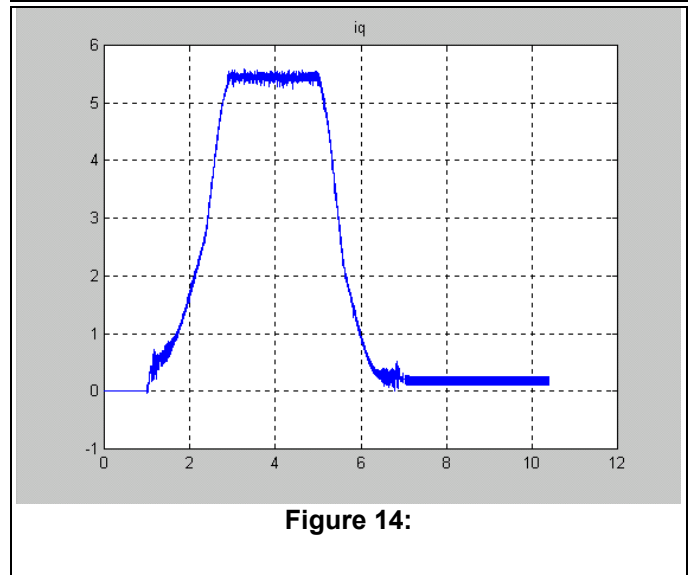
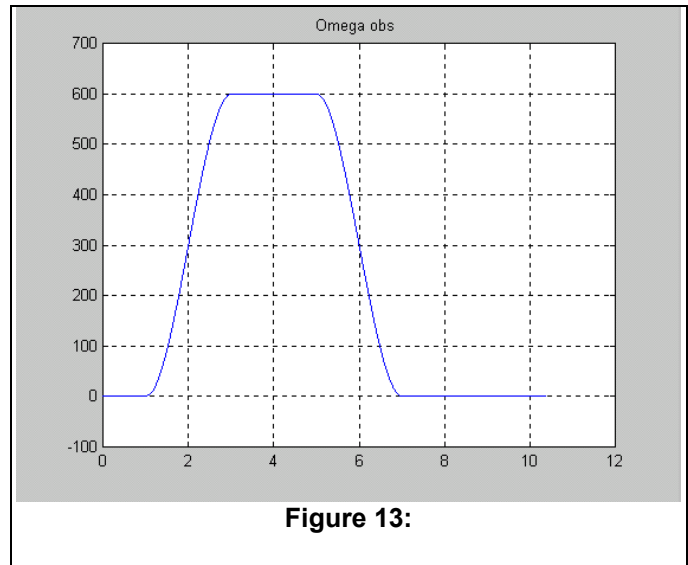
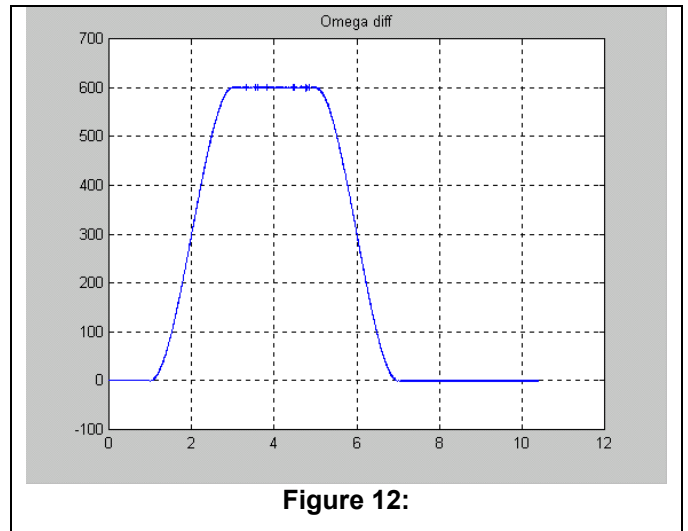


the Simulink blocks of the motor/amplifier.

An experimental run in which the speed was brought up from zero to 600 rads/sec and back to zero is shown in the figure 12 below. The speed was computed by differentiating the feedback from the optical encoder.

Figure 13 shows the speed computed using a speed observer. Figure 14 shows a plot of the quadrature current that was needed to make the speed runs shown above.

The point here is to show how easy it is to take the SIMULINK blocks from the Library and turn them into a simulation and then into a real-time implementation.



INDUCTION MOTOR

The third motor for which a Library of simulation models have been developed is the induction motor. A standard two-phase equivalent model of the induction motor is given by [32]

where

$$\frac{d\theta}{dt} = \omega \quad (39)$$

$$\frac{d\omega}{dt} = \mu(i_{Sb}\psi_{Ra} - i_{Sa}\psi_{Rb}) - (D/J)\omega - \tau_L/J \quad (40)$$

$$\frac{d\psi_{Ra}}{dt} = -\eta\psi_{Ra} - n_p\omega\psi_{Rb} + \eta Mi_{Sa} \quad (40)$$

$$\frac{d\psi_{Rb}}{dt} = -\eta\psi_{Rb} - n_p\omega\psi_{Ra} + \eta Mi_{Sb} \quad (41)$$

$$\frac{di_{Sa}}{dt} = \eta\beta\psi_{Ra} + \beta n_p\omega\psi_{Rb} - \gamma i_{Sa} + u_{Sa}/\sigma L_S \quad (42)$$

$$\frac{di_{Sb}}{dt} = \eta\beta\psi_{Rb} - \beta n_p\omega\psi_{Ra} - \gamma i_{Sb} + u_{Sb}/\sigma L_S \quad (43)$$

$$\text{where } \eta = \frac{R_R}{L_R}, \beta = \frac{M}{\sigma L_R L_S}, \mu = \frac{n_p M}{J L_R}, \gamma = \frac{M^2 R_R}{\sigma L_R^2 L_S} + \frac{R_S}{\sigma L_S} \quad (44)$$

Then letting

$$p = \tan^{-1}\left(\frac{\psi_{Rb}}{\psi_{Ra}}\right) \quad (45)$$

$$\psi_d = \sqrt{\psi_{Ra}^2 + \psi_{Rb}^2} \quad (46)$$

and defining the dq transformation as

$$\begin{bmatrix} u_d \\ u_q \end{bmatrix} = \begin{bmatrix} \cos(\rho) & \sin(\rho) \\ -\sin(\rho) & \cos(\rho) \end{bmatrix} \begin{bmatrix} u_{Sa} \\ u_{Sb} \end{bmatrix} \quad (47)$$

$$\begin{bmatrix} i_d \\ i_q \end{bmatrix} = \begin{bmatrix} \cos(\rho) & \sin(\rho) \\ -\sin(\rho) & \cos(\rho) \end{bmatrix} \begin{bmatrix} i_{Sa} \\ i_{Sb} \end{bmatrix} \quad (48)$$

The equations of the motor may be written in this new coordinate system as

$$\frac{d\theta}{dt} = \omega \quad (49)$$

$$\frac{d\omega}{dt} = \mu\psi_d i_q - (D/J)\omega - \tau_L/J \quad (50)$$

$$\frac{d\psi_d}{dt} = -\eta\psi_d + \eta Mi_d \quad (51)$$

$$\frac{di_d}{dt} = -\lambda i_d + (\eta M / \sigma L_R L_S)\psi_d + n_p\omega i_q + \eta Mi_q^2 / \psi_d + u_d / \sigma L_S \quad (52)$$

$$\frac{di_q}{dt} = -\gamma i_q - (M / \sigma L_R L_S)n_p\omega\psi_d - n_p\omega i_d - \eta Mi_q i_d / \psi_d + u_q / \sigma L_S \quad (53)$$

$$\frac{d\rho}{dt} = n_p\omega + \eta Mi_q / \psi_d \quad (54)$$

A standard approach is to use PI current controllers of the form

$$v_d = K_{dI} \int_0^t (i_{dr} - i_d) dt + K_{dP} (i_{dr} - i_d) \quad (55)$$

$$v_q = K_{qI} \int_0^t (i_{qr} - i_q) dt + K_{qP} (i_{qr} - i_q) \quad (56)$$

resulting in the reduced order model

$$\frac{d\theta}{dt} = \omega \quad (57)$$

$$\frac{d\omega}{dt} = \mu\psi_d i_{qr} - (D/J)\omega - \tau_L/J \quad (58)$$

$$\frac{d\psi_d}{dt} = -\eta\psi_d + \eta Mi_{dr} \quad (59)$$

$$\frac{d\rho}{dt} = n_p\omega + \eta Mi_q / \psi_d \quad (60)$$

The dq current references are chosen as

$$i_{qr} = \frac{\tau_{ref}}{\mu\psi_d} \quad (61)$$

$$i_{dr} = K_{\psi I} \int_0^t (\psi_{dref} - \psi_d) dt + K_{\psi P} (\psi_{dref} - \psi_d) \quad (62)$$

and flux magnitude $\hat{\psi}_d$ and angle $\hat{\rho}$ are estimated using

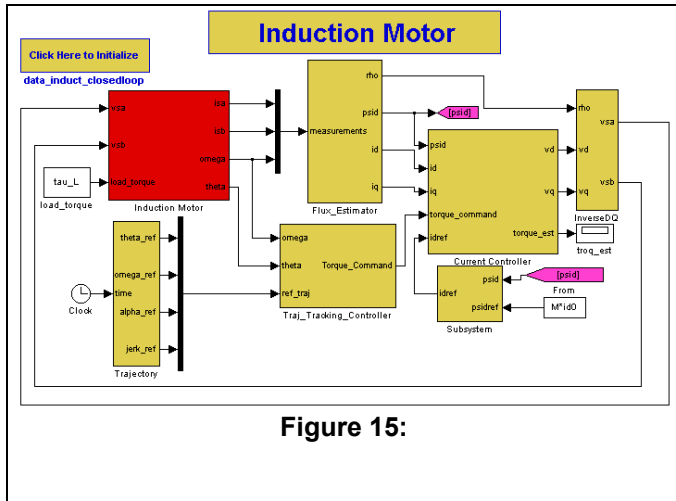


Figure 15:

$$\begin{aligned} \frac{d\hat{\rho}}{dt} &= n_p \omega + \eta M \hat{i}_q / \hat{\psi}_d \\ &= n_p \omega + \eta M (-i_{sa} \sin(\hat{\rho}) + i_{sb} \cos(\hat{\rho})) / \hat{\psi}_d \end{aligned} \quad (63)$$

$$\begin{aligned} \frac{d\hat{\psi}_d}{dt} &= -\eta \hat{\psi}_d + \eta M \hat{i}_d \\ &= -\eta \hat{\psi}_d + \eta M (i_{sa} \cos(\hat{\rho}) + i_{sb} \sin(\hat{\rho})) \end{aligned} \quad (64)$$

The top level of the model making up this induction motor controller is shown below.

CONCLUSIONS AND FURTHER WORK

This paper outlines the development of a library of SIMULINK blocks that can be used to implement state of the art controllers for switched reluctance, PM synchronous and Induction motors. The objective of this work is to provide developer of HEV controllers a readily accessible set of basic control algorithms for real-time implementation. Future work will concentrate on encoderless control schemes for the SR and Induction motors, parameter identification schemes for the induction and PM synchronous motors and power electronic control schemes including Carrier-based pulse width modulation (PWM), Space vector PWM and Harmonic elimination based PWM.

CONTACTS

John Chiasson received his Bachelor's Degree in Mathematics from the University of Arizona, his Master's Degree in Electrical Engineering from Washington State University and his PhD in Controls from the University of Minnesota. His work in industry started at Boeing Aerospace from 1978 to 1979 working in the area of Flight Controls, Guidance and Navigation. From 1982-1983 he worked at Control Data in the area of CAD systems and from 1984-1985 he worked at Honeywell Science and Technology Center in the area of inertial navigation. His latest stint in industry was from 1996-

1999 at ABB Daimler-Benz Transportation where he worked in the development of AC motor propulsion systems, real-time simulators and the stability analysis of AC propulsion systems. He has held academic positions at Purdue University and the University of Pittsburgh and, since 1999, has been on the faculty of Electrical and Computer Engineering at the University of Tennessee. He does research in the areas of the control of electric motor drives, multilevel converters, hybrid electric vehicles as well as mathematical systems theory. He is a participating faculty member of the Graduate Automotive Technology Education (GATE) Center at UT, and one of the advisors for the FutureTruck 2002 competition. Dr. Chiasson is a Member of the IEEE, and a member of the IEEE Control Systems Society, IEEE Power Electronics Society, and IEEE Industrial Electronics Society. His email address is chiasson@utk.edu

Leon M. Tolbert received the B.E.E., M.S., and Ph.D. degrees in electrical engineering from the Georgia Institute of Technology. He joined the Engineering Division of Lockheed Martin Energy Systems in 1991 and has worked on several electrical distribution and power quality projects at the three U.S. Department of Energy plants in Oak Ridge, Tennessee. In 1997, he became a Research Engineer in the Power Electronics and Electric Machinery Research Center (PEEMRC) at the Oak Ridge National Laboratory. He was appointed as an assistant professor in the Department of Electrical and Computer Engineering at The University of Tennessee in Knoxville in 1999. He does research in the areas of electric power conversion, motor drives, multilevel converters, hybrid electric vehicles, and power quality. He is also a participating faculty member of the Graduate Automotive Technology Education (GATE) Center at UT. He is an adjunct participant at the Oak Ridge National Laboratory and conducts joint research at the National Transportation Research Center (NTRC). Leon's e-mail address is tolbert@utk.edu.

REFERENCES

1. Opal RT Technologies, RT-LAB Real Time Laboratory Users Manual Version 3.4, Montreal Canada, 2000.
2. Vas, Peter, *Sensorless Vector and Direct Torque Control*, Oxford Press, 1998. (See chapter 5)
3. Lumsdaine, Andrew and Jeffrey Lang, "State Observers for Variable-Reluctance Motors", IEEE Transactions on Industrial Electronics, Vol. 37, No. 2, April 1990.
4. Harris, W.D. and Jeffrey Lang, "A Simple Motion Estimator for Variable-Reluctance Motors" IEEE Transactions on Industry Applications, Vol. 26, No. 2, March/April 1990.
5. Ilic-Spong, M., R. Marino, S. Peresada and D. G. Taylor, "Feedback Linearizing Control of Switched Reluctance Motors", IEEE Transactions on Automatic Control, Vol. 32, No. 5, May 1987.
6. Taylor, D.G., M.J. Woolley and M. Ilic, "Design and Implementation of a Linearizing and Decoupling Feedback Transformation for Switched Reluctance

- Motors", The 17th Symposium on Incremental Motion Control Systems and Devices, Champaign, IL, pp. 173-184, June 1988.
7. Taylor, D.G., "An Experimental Study on Composite Control of Switched Reluctance Motors", IEEE Control Systems, February 1991.
 8. Wallace, R.S. and D.G. Taylor, "A Balanced Commutator for Switched Reluctance Motors to Reduce Torque Ripple", IEEE Transactions on Power Electronics, Vol. 7, No. 4, October 1992
 9. Rehman, S.U., David G. Taylor, "Piecewise Modeling and Optimal Commutation of Switched Reluctance Motors," Proceedings of the IEEE International Symposium on Industrial Electronics, pp. 266-271, 1995.
 10. Rehman, S.U., David G. Taylor, "Issues in Position Estimation of SR Motors", Proceedings of the 27th IEEE Power Electronics Specialists Conference, pp.337-343, 1996.
 11. Kim, C-H, I-J Ha, "A New Approach to Feedback-Linearizing Control of Variable Reluctance Motors for Direct-Drive Applications", IEEE Transactions on Control Systems Technology, Vol. 4, No. 4, July 1996.
 12. Milman, R. and S.A. Bortoff, "Observer-Based Adaptive Control of a Variable Reluctance Motor: Experimental Results", IEEE Transactions on Control Systems Technology, Vol. 7, No. 5, September 1999.
 13. Holling, G.H., "The Sensorless Control of Variable Switched Reluctance Motors", Proceedings of the American Control Conference, June 1998.
 14. Rajashekara, K., A. Kawamura, K. Matsuse, Editors, *Sensorless Control of AC Motor Drives - Speed and Position Sensorless Operation*, IEEE Press, 1996.
 15. Husain, I. and M. Ehsani, "Rotor Position Sensing in Switched Reluctance Motor Drives by Measuring Mutually Induced Voltages", IEEE Transactions on Industry Applications, vol. 30, No. 3, pp. 665-672.
 16. Ehsani, M., I. Husain, A. Kulkarni, "Elimination of Discrete Position Sensor and Current Sensor in Switched Reluctance Motor Drives", IEEE IAS Annual Meeting, 1991.
 17. Ehsani, M. and K.R. Ramani, "Direct Control Strategies Based on Sensing Inductance in Switched Reluctance Motors", IEEE Transactions on Power Electronics, Vol. 11, No. 1, 1996.
 18. Husain, I. and M. Ehsani, "Torque Ripple Minimization in Switched Reluctance Motor Drives by PWM Current Control", IEEE Transactions on Power Electronics, Vol. 11, No. 1, 1996.
 19. Fahimi, B., G. Suresh, M. Ehsani, "Design Considerations of Switched Reluctance Motors: Vibration and Control Issues", IEEE IAS Annual Meeting, 1999.
 20. Garrigan, N.R., W.L. Soong, C.M. Stephens, A. Storace and T.A. Lipo, "Radial Force Characteristics of a Switched Reluctance Machine", IEEE IAS Annual Meeting, 1999.
 21. Lyons, J., S. MacMinn and M. Preston, "Flux/Current Methods for SRM Rotor Position Estimation, IEEE IAS Annual Meeting", 1991.
 22. Laurent, P., M. Gabsi, B. Multon, "Sensorless Rotor Position Analysis Using Resonant Method for Switched Reluctance Motors", IEEE IAS Annual Meeting}, 1993.
 23. Saha, S., K. Ochiai, T. Kosaka, N. Matsui, and Y. Takeda, "Developing a Sensorless Approach for Switched Reluctance Motors from a New Analytical Model", IEEE IAS Annual Meeting, 1999.
 24. Acarnley, P.P., R.J. Hill and C.W. Hooper, "Detection of Rotor Position in Stepping and Switched Motors by Monitoring of Current Waveforms", IEEE Transactions on Industrial Electronics, Vol. IE-32, pp. 215-222, August 1985.
 25. Sastry, S. and M. Bodson, *Adaptive Control: Stability, Convergence, and Robustness*, Prentice Hall, 1989.
 26. Ljung, L., *System Identification: Theory for the User*, Prentice Hall, 1987.
 27. Miller, T.J.E., *Switched Reluctance Motors and Their Control*, Oxford Science Publications, 1993.
 28. Panda, D. and V. Ramanarayanan, "Effect of Mutual Inductance on Steady-State Performance and Position Estimation of Switched Reluctance Motor Drive", IEEE IAS Annual Meeting, 1999.
 29. "Technical Assessment of Switched Reluctance Drives for Application in Electric and Hybrid Vehicles", DOE document prepared by EA Engineering, Science, and Technology, Inc.
 30. Cheok, A.D., and N. Ertugrul, "High Robustness of an SR Motor Angle Estimation Algorithm using Fuzzy Predictive Filters and Heuristic Knowledge Based Rules", IEEE Transactions on Industrial Electronics, Vol. 46, No. 5, Oct. 1999.
 31. Bodson, M., Chiasson, J.N., Novotnak, R.T., & Rekowski R.B., "High-Performance Nonlinear Feedback Control of a Permanent Magnet Stepper Motor," IEEE Trans. on Control Systems Technology, vol. 1, no. 1., 1993, pp. 5 - 14.
 32. Leonhard, W., *Control of Electrical Drives*, Springer Verlag, Berlin, 1990.
 33. Blauch, A., Bodson, M., & Chiasson, J., "High-Speed Parameter Estimation of Stepper Motors," IEEE Trans. on Control Systems Technology, vol. 1, no. 4, 1993, pp. 270-279.
 34. Bodson, M., Chiasson J., & Novotnak, R.T., "A Systematic Approach to Selecting Optimal Flux References in Induction Motors," IEEE Trans. Control Systems Technology, vol. 3, no. 4, 1995, pp. 388-397.
 35. Lawler, J.S., J.M. Bailey and J.W. McKeever, "Extended Constant Power Speed Range of the Brushless DC Motor Through Dual Mode Inverter Control", Oak Ridge National Lab Report, ORNL/TM-2000/130, 2000.
 36. Verl, A. and M. Bodson, "Torque Maximization for Permanent Magnet Synchronous Motors", IEEE Trans. on Control Systems Technology, vol. 6, no. 6, 1998, pp. 740-745.
 37. Marc Bodson, John N. Chiasson and Leon M. Tolbert, "A Complete Characterization of Torque Maximization of Permanent Magnet Non-Salient

Synchronous Motors," *IEEE American Controls Conference*, June 25-27, 2001, Arlington, Virginia.

38. John N. Chiasson and Leon M. Tolbert, "High Performance Motion Control of a Switched

Reluctance Motor," *IEEE International Electric Machine Drives Conference*, June 17-20, 2001, Cambridge, Massachusetts, pp. 425-429.